THE JOURNAL OF PHYSICAL CHEMISTRY A

Article

pubs.acs.org/JPCA

The Hydration Effect and Selectivity of Alkali Metal Ions on Poly(ethylene glycol) Models in Cyclic and Linear Topology

Lokendra Poudel,[†] Rudolf Podgornik,[‡,§] and Wai-Yim Ching*[,†]

[†]Department of Physics and Astronomy, University of Missouri-Kansas City, Kansas City, Missouri 64110, United States

[‡]Department of Theoretical Physics, J. Stefan Institute, SI-1000 Ljubljana, Slovenia

[§]Department of Physics, Faculty of Mathematics and Physics, University of Ljubljana, SI-1000 Ljubljana, Slovenia

Supporting Information

ABSTRACT: The effects of hydration and alkali metal ion (K^+, Na^+, Li^+) bonding to two structural variants of poly(ethylene glycol) (PEG), viz., a cyclic (18-crown-6) configuration and a linear chain model with two different lengths, are studied by ab initio density functional theory calculations. A total of 24 structural models are constructed, with different conformations of the PEG chain and its molecular environment. Detailed comparisons of the results enable us to obtain conclusive evidence on the effects of the different components of the solution environment on the PEG structural variants in terms of the binding energy, partial charge distribution, solvation effect, interfacial hydrogen bonding, and cohesion between different structural units in the system composed of PEG, alkali metal ions, and water. On the basis of these comprehensive and precise comparisons, we conclude that the ion−PEG interaction is strongly influenced by the presence of solvent and that the charge transfer in the PEG complex depends crucially on its topology, the type of alkali metal ion, and the solvent. The interaction between alkali metal ions in the two PEG models does not always scale with the ion size but depends on their local environment.

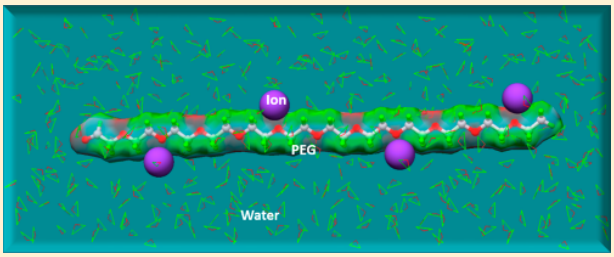

1. INTRODUCTION

Poly(ethylene glycol) (PEG, $-[CH_2-CH_2-O-]_nCH_2-CH_2-OH$) and poly(ethylene oxide) (PEO, $-[CH_2-CH_2-O-]_n$) are polyether compounds of great biological interest with often-noted anomalous physical properties,[1] of which the most important one is the solubility in aqueous solutions over a wide range of concentrations, molecular weights, temperatures, and pressures.[2−4] Because of their properties, aqueous solutions of PEG have been used widely as matrices for embedding, antifreezes, lubricants for medical devices, and food additives. On the other hand, covalent PEG grafting or non-covalent coating of molecular and nanoparticle surfaces enables steric stabilization, conferring "stealth" properties with respect to the host's immune defense system that are highly desirable in gene therapy and drug delivery for pharmaceutical applications.[5] Because PEG is virtually immiscible with other biopolymers such as proteins and/or nucleic acids, it is also often used as a crystallization agent and precipitant,[6,7] acting as an osmoticant for the phase-separated subphase and thus directly enabling the quantification of macromolecular interactions in the osmotic-stress method.[8] In this context, its equation of state connecting the osmotic pressure of a PEG solution and its concentration has been studied in great detail.[9]

The solubility of PEG in water is generally attributed to hydrogen bonding between water molecules and oxygens along the PEG backbone, which is a consequence of a good structural fit between water and the polymer.[10] It has been reported that PEG can at least to some extent retain the helical structure observed in crystals and that a related structure observed in aqueous solution can be attributed to hydrogen bonding between water and PEG.[11] As a consequence, PEG might coordinate cations in an electrolyte solution by forming compact helical crown ether-like structures that would display polyelectrolyte-like properties, a hypothesis made plausible by small-angle neutron scattering on PEG solutions[12] but not directly confirmed by the equation of state experiments.[9] Additional details of the PEG behavior in aqueous solutions have been investigated by molecular mechanics (MM), molecular dynamics (MD), and Monte Carlo (MC) simulation techniques[13−16] based on specific force fields[17,18] or generic CHARMM parametrizations,[19] but only a few ab initio quantum calculations have been set up to study PEG−water interactions, typically using only a small number of water molecules.[20] Classical simulations cannot provide quantitative information on the partial charge distributions, nor can they furnish a quantitative description of hydrogen bonds (HBs) independent of force field parametrizations. Despite the long history of the study of PEG in solution, the important issue of accurately accounting for PEG−ion, PEG−water, and water−water hydrogen-bonding interactions, which are coupled

Received: April 29, 2017
Revised: May 25, 2017
Published: May 29, 2017

DOI: 10.1021/acs.jpca.7b04061
J. Phys. Chem. A 2017, 121, 4721−4731

cooperatively in PEG aqueous solutions, is still missing. For a deeper understanding of the solution behavior of PEG, ab initio calculations with a sufficiently large number of water molecules in different ionic environments are therefore highly desirable.

In addition to the solution behavior context, PEG has become increasingly relevant also in nanopore-based sensors that exploit the variation of current through ion-conducting aqueous pores[11] as a consequence of passive and/or forced partitioning of PEG into the pore.[21] The interaction between PEG and the pore in, e.g., the α-hemolysin membrane channel, can then be used as a proxy for understanding the general interactions of polymers with the nanopore, as mediated by the aqueous solvent and the dissolved electrolyte, and to develop advanced models for polymer confinement within the pore.[22] Quite surprisingly, the response of PEG to an external voltage suggests that the molecules of PEG in aqueous potassium salt solutions at concentrations greater than 1 M can display polyelectrolyte properties, carrying charges[23] and in fact entering the nanopore dressed by cations such as K^+.[22] Later experimental studies focused on the effect of different alkali ions on the neutral versus polyelectrolyte behavior of PEG, confirming that Na^+, K^+, Rb^+, and Cs^+ but not Li^+ can induce the polyelectrolyte behavior.[24] Furthermore, detailed MD simulations additionally elucidated the nature of the cation binding,[18] indicating that a single K^+ cation can coordinate with four PEG monomers in a crown ether-like structure,[19] similar to the one claimed to exist in the bulk solution, and that the solvent-induced PEG−ion interaction strongly influences also the ion selectivity of the PEG.[13−16] Again, only a few ab initio calculations exist to elucidate the molecular details of the PEG−ion interactions, and even those were mostly performed in the gas phase.[25−28]

To further elucidate the molecular details of the PEG−water and PEG−ion interactions, possibly leading to observed polyelectrolyte effects, we have specifically designed 24 PEG models based on the linear and crown ether variants in the presence of aqueous solvent with alkali metal ions and applied a combination of two ab initio quantum calculation methods based on density functional theory (DFT).[29,30] This strategy offers the best balance between accuracy and feasibility of realistic simulation under different scenarios, thereby providing specific answers to some unresolved issues in PEG research, which are difficult to sort out by either classical molecular simulation or pure laboratory experimentation. Therefore, the objective of this study is to determine precisely the role of water in the selectivity of cyclic and linear PEG for alkali metal ions using ab initio calculations.

In what follows, we first describe the design and construction of the 24 PEG models in specific environments followed by the methods used in the calculation. Our results provide a detailed molecular understanding of the influence of the type of alkali metal ion and its role in binding to PEG with or without the presence of water. We report gas-phase and solvated affinities of K^+, Na^+, and Li^+ with two different topologies, the cyclic crown ether and linear forms of PEG. In the linear chain case, we further investigate the effect of the length of the PEG chain with alkali metal ions in the presence of water or in vacuo. This comprehensive study of the electronic structure and interatomic bonding, especially the hydrogen bonding, energetics, and interactions between different structural motifs in the well-designed PEG models, clarifies some existing confusions in PEG research. In conjunction with experimental data, our findings can be used to further advance the understanding of the ionic solution behavior of PEG.

2. MODELING AND SIMULATION

We start with the structures of cyclic PEG 18-crown-6 (18c6) taken from PubChem (ID 28557) and linear PEG with $n = 6$ constructed using DS ViewerPro software. For meaningful comparison between the cyclic and linear configurations of PEG, we used an equal number of atoms by modifying the end groups of the linear PEG (see Figure 1). To study the effect of topology and chain length in different environments and to ascertain the specific influence of the water and alkali metal ions (K^+, Na^+, and Li^+) on these structures, a series of models based on the cyclic and linear structures were designed and fully optimized for ab initio calculations (see Figure 2). First, we constructed eight periodic models each for cyclic and linear PEG, which are listed in Table 1, labeled as A1−A8 and B1−B8, respectively. Half of these models were explicitly solvated with 200 water molecules and half of them with no water molecules, with or without the alkali metal ions. For each pair of models, there was only one specific difference in the structural arrangement, which enabled us to pin down exactly the source of difference in the results. This is extremely important because none of the past studies could reveal the precise reason for the differences, depending on the mixture of complexity in structure and the interconnected interactions between metal ions and solvent, resulting in vague or even contradictory conclusions. We also constructed eight additional linear models with the length of the chain doubled. The numbers of ions and water molecules were also doubled to ascertain the effects of the chain length. These models are labeled as C1−C8 in Table 1. The last three models (C6−C8) are the largest models we studied, with 1288 atoms in the cell.

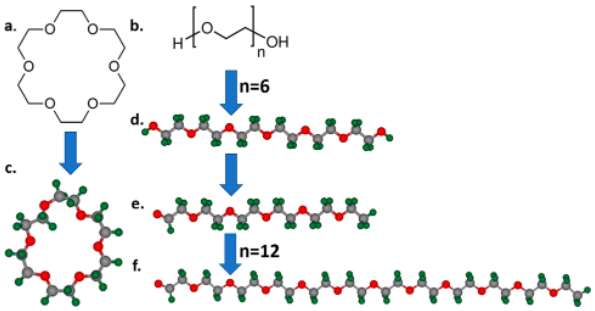

Figure 1. Structures of 18-crown-6 (18c6) and poly(ethylene glycol) (PEG). (a, b) Line structures of (a) 18c6 and (b) PEG. (c−f) Ball-and-stick representations of (c) 18c6, (d) PEG with $n = 6$, (e) modification of PEG with $n = 6$ at the terminals to obtain the same number of atoms as in (c), and (f) PEG with $n = 12$ (i.e., double the chain length of (e)).

Our overarching goal was a comprehensive study of structural variations, solvent effects, and selectivity for alkali metal ions and PEG and the fundamental electronic interactions between them. For the initial configuration, before the full relaxation, we added two alkali metal ions to each of the cyclic and linear PEG models. For the cyclic case, one metal ion was put at the center of the crown and the other above it. For the linear case, one metal ion was put near the center of the chain and the other at the end of the chain. We then added 200 water molecules for the solvated models, using the TIP3P water

DOI: 10.1021/acs.jpca.7b04061
J. Phys. Chem. A 2017, 121, 4721−4731

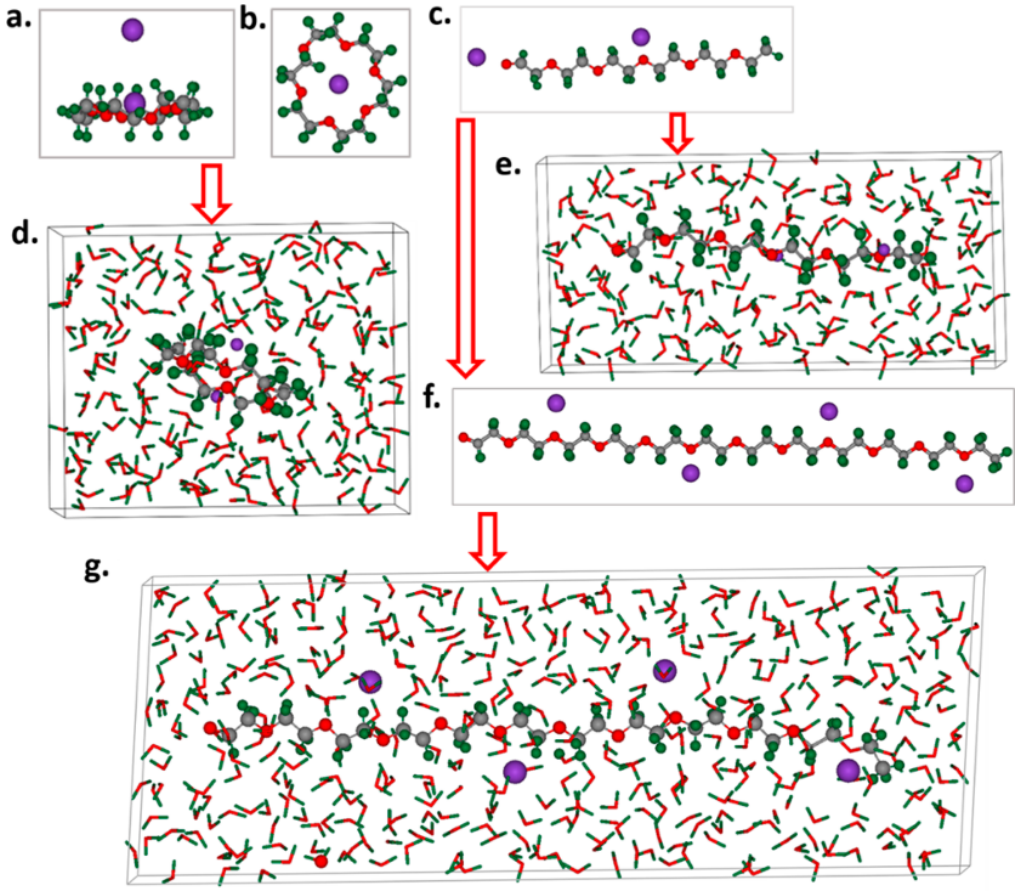

Figure 2. Relaxed structures of 18c6 and linear PEG with alkali ions (M^+ = K^+, Na^+, Li^+). (a) Planar view of dry 18c6 with M^+. (b) Vertical view of 18c6 with M^+. (c) Dry phase of linear PEG with n = 6 (LP-6) with M^+. (d) Solvated 18c6 with M^+. (e) Solvated LP-6 with M^+. (f) Dry phase of linear PEG with n = 12 (LP-12) with M^+. (g) Solvated LP-12 with M^+. The ball-and-stick models denote 18c6 and linear PEG, the thin sticks represent water molecules, and purple balls represent alkali ions.

Table 1. The 24 PEG Models[a]

name	cyclic PEG	name	linear PEG	name	double linear PEG
A1	CP	B1	LP	C1	2(LP)
A2	CP+2K	B2	LP+2K	C2	2(LP+2K)
A3	CP+2Na	B3	LP+2Na	C3	2(LP+2Na)
A4	CP+2Li	B4	LP+2Li	C4	2(LP+2Li)
A5	CP+200H_2O	B5	LP+200H_2O	C5	2(LP+200H_2O)
A6	CP+2K+200H_2O	B6	LP+2K+200H_2O	C6	2(LP+2K+200H_2O)
A7	CP+2Na+200H_2O	B7	LP+2Na+200H_2O	C7	2(LP+2Na+200H_2O)
A8	CP+2Li+200H_2O	B8	LP+2Li+200H_2O	C8	2(LP+2Li+200H_2O)

[a]The left pair of columns originates from the cyclic PEG structure, the center pair of columns from the linear PEG structure, and the right pair of columns from linear PEG with double chain length. The environment of each pair in the row is the same.

model[31] as implemented in the Chimera software.[32] The TIP3P water model is a simple three-site model with three interaction sites, corresponding to the three atoms of the water molecule. The O−H bond length and H−O−H bond angle were set to 0.95 Å and 104.52°, respectively. The water molecules surrounding the PEG structure were added using Amber Tools as incorporated in the Chimera software. There were a total of 644 and 44 atoms in the solvated and dry PEG models with metal ions, respectively. Furthermore, the sizes of the models were exactly doubled (1288 in the solvated and 88 in the gas phase) in the double-length-chain cases. It should be noted that the numbers of alkali ions and water molecules were the same in all of the PEG models, even though their positions and orientation may differ. In addition, all 24 models with periodic boundary conditions were fully relaxed using the Vienna Ab Initio Simulation Package (VASP)[33] with high accuracy. The precise pairwise comparisons among these models enabled us to extract the information needed to clarify the many aspects of the PEG behavior in ionic solutions.

3. COMPUTATIONAL METHODS

For structural relaxation of the PEG models and their total energies (TEs) we used VASP, which is DFT-based[29,30] and has been highly effective for geometry optimization. We used the

DOI: 10.1021/acs.jpca.7b04061
J. Phys. Chem. A 2017, 121, 4721−4731

Table 2. Calculated Total Energies (TEs) and Binding Energies (BEs) for Gas-Phase Models of Cyclic (18c6) PEG and Linear PEG with Metal Ions

		TEs in structural units (eV)					TEs in structural units (eV)		
18c6 model	TE (eV)	18c6	ions	BE (eV)	linear model	TE (eV)	LP	ions	BE (eV)
A1	−234.5524	–	–	–	B1	−234.5432	–	–	–
A2	−236.4186	−234.4062	−0.8870	−1.1254	B2	−235.3223	−234.4828	−0.1618	−0.6777
A3	−236.5812	−234.2312	−1.1442	−1.2058	B3	−235.2651	−234.0226	−0.1130	−1.1295
A4	−237.1601	−234.3748	−1.3807	−1.4046	B4	−238.3188	−234.4637	−0.1177	−3.3774

projector-augmented wave method with the Perdew−Burke−Ernzerhof (PBE) potential[34] for the exchange−correlation functional within the generalized gradient approximation. A relatively high energy cutoff of 500 eV was used, with the electronic convergence criterion set at 10^{-5} eV and force convergence at 10^{-3} eV/Å. Since a large supercell was used, a single **k**-point calculation at the zone center was sufficient. Similar relaxation for other complex systems was successfully demonstrated in our recent publications.[35−38] The binding energy (BE) for each model was calculated according to the simple equation

$$\mathrm{BE(model\ i)} = \mathrm{TE(model\ i)} - \sum_{j} \mathrm{TE(component\ j\ for\ model\ i)} \quad (1)$$

where j stands for the structural units PEG, metal ions, and water at the instantaneous position of model i. It should be pointed out that each structural unit such as water contains individual atoms that were considered to be frozen in order to focus only on the interfacial binding energy between these units.

The electronic properties of the PEG models were calculated using the ab initio orthogonal linear combination of atomic orbitals (OLCAO) method[39] with the VASP-relaxed structures as input. There are many advantages of the all-electron OLCAO method with local atomic orbitals in the basis expansion. These include flexibility in basis choice, lower computational cost, and easy analysis of results using the Mullikan scheme, making it therefore an extremely efficient methodology for electronic structure calculations on large, complex systems. The electronic structures include partial charge distributions and interatomic bonding. In the present calculation for the PEG models, a full basis (FB) was used for the determination of the self-consistent potential and a minimum basis (MB) for the calculation of partial charge (PC) and bond order (BO) values. The MB for each atom consists of the core orbitals and a shell of occupied valence orbitals. The FB further includes the next shell of unoccupied orbitals. More details can be found in ref 39. In combination with VASP, the OLCAO method has been successfully employed in the study of many complex inorganic[40−42] and organic crystals[43] as well as biomolecules such as DNA,[36,37] collagen,[44] proteins,[35] and drug−DNA complexes.[38]

The effective charge (Q^*_α) on each atom α and BO value $\rho_{\alpha\beta}$ (in units of electrons) for each pair of atoms α and β were calculated according to the Mulliken scheme[45] with a minimum basis:

$$Q^*_\alpha = \sum_i \sum_{n\ (\mathrm{occ})} \sum_{j,\beta} C^{n*}_{i\alpha} C^{n}_{j\beta} S_{i\alpha,j\beta} \quad (2)$$

$$Q_{\alpha\beta} = \sum_{n\ (\mathrm{occ})} \sum_{i,j} C^{n*}_{i\alpha} C^{n}_{j\beta} S_{i\alpha,j\beta} \quad (3)$$

where $C^n_{j\beta}$ are the eigenvector coefficients of the nth occupied state, jth orbital, and β^{th} atom and the $S_{i\alpha,j\beta}$ are the corresponding overlap integrals.

In the present work, whereas Q^* and BO were calculated using the MB, the self-consistent potential and electronic structure calculations used the FB, which was carefully constructed and well-tested for each atom within the database of the OLCAO package.[39] The deviation of Q^* from the neutral atom value, Q_0 (i.e., the charge transfer, $\Delta Q = Q_0 - Q^*$) is the partial charge (PC) on that atom (i.e., negative ΔQ corresponds to gain of electrons or electronegative, and positive ΔQ corresponds to loss of electrons or electropositive). The bond order quantifies the relative strengths of intra- and intermolecular bonds and generally scales with the bond length (BL) but also depends on the local environment of the bonding pair. Accurate quantification of bonding characteristics based upon quantum-mechanical calculations and their relationship with electronic structure can then serve as a platform for understanding the structure of complex systems. It should be noted that in all of the DFT calculations, the entire cell or the system was charge neutral. However, the PC on each atom calculated according to eq 2 provides the quantitative information on charge transfer from one atom to another atom. Adding these PCs within each structural unit as defined in Table 1 and making pairwise comparisons allows much more detailed information to be obtained for a complex multicomponent system. The same strategy can be applied to the BO values from eq 3. These will be illustrated later in section 4 when specific results are discussed. The BO is particularly important for the relative contributions of hydrogen bonding and ionic bonding, which have not yet been assessed for the PEG models. The total bond order (TBO) is the cumulative BO from all unique bond pairs in the total structure, and the partial bond order (PBO) is the cumulative BO from all of the bond pairs from certain structural units. It is well-known that the Mulliken scheme used in the present calculation is basis-set-dependent and thus can be very different in different computational packages. We used the well-tested MB set within the OLCAO package to perform the calculations for PC and bond order. There are other more accurate methods, such as the Bader molecular scheme based on the charge density distribution in three dimensions, instead of the overlap population of the wave functions in the Mulliken scheme. Bader analysis is generally restricted to smaller molecules or crystals and would be too onerous for more complex multicomponent systems, where topological analysis to obtain the charge density distribution can be overwhelming. This is exactly the reason that we had to design 24 models in order to make pairwise comparisons for a specific conclusion without the shortcomings of the Mulliken scheme.

DOI: 10.1021/acs.jpca.7b04061
J. Phys. Chem. A 2017, 121, 4721−4731

Table 3. Calculated Total Energies (TEs) and Binding Energies (BEs) for Solvated Models of 18c6 and Linear PEG with Metal Ions

		TEs in structural units (eV)					TEs in structural units (eV)			
18c6 model	TE (eV)	18c6	ions	water	BE (eV)	linear model	TE (eV)	LP	ions	water	BE (eV)
A5	−3184.3977	−234.4497	–	−2948.8967	−1.0513	B5	−3182.7793	−234.4251	–	−2947.7245	−0.6297
A6	−3190.2687	−234.1577	−0.9337	−2947.8674	−7.3099	B6	−3188.8141	−230.1472	−0.1639	−2940.5432	−17.9598
A7	−3189.1428	−234.3194	−1.2001	−2947.1464	−6.4769	B7	−3189.0217	−230.1383	−0.1133	−2941.8297	−16.9404
A8	−3187.9212	−234.4209	−1.4494	−2945.7396	−6.3113	B8	−3190.4448	−230.2005	−0.1141	−2944.7405	−15.3897

4. RESULTS AND DISCUSSION

We now present the calculated results for each pair of models in which only one of the descriptors is different, such as dry versus solvated, crown versus linear, or metal versus no metal, and observations of the trends for each case with respect to the alkali ion sequence K^+, Na^+, and Li^+. Such pairwise comparisons are not an easy matter and must be done carefully because of many possible combinations and their interdependence.

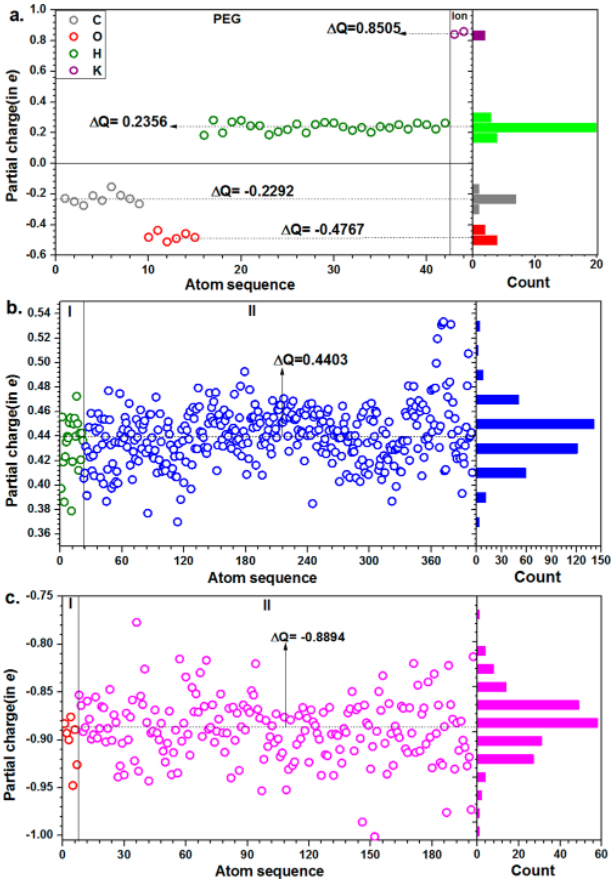

Figure 3. Calculated atomic partial charge distributions in solvated model A6 (18c6+2K+200H_2O): (a) PEG with K^+ ions; (b) H atoms in water molecules; (c) O atoms in water molecules. The left panels represent the distributions of partial charge as scatter plots and the right panels as histogram plots. In (b) and (c), regions I and II represent those atoms forming HBs with PEG and those forming HBs between water molecules, respectively. The *y*-axis scales in (a), (b), and (c) are different for better visual juxtaposition, showing the scattered distribution depending on the local environment. The dashed lines and arrows denote the average values of the PC Δ*Q* in units of electrons.

Table 4. Net Partial Charges (PCs) in Different Structural Parts of Gas-Phase Models

	PCs in structural units (electrons)			PCs in structural units (electrons)	
18c6 model	18c6	ions	linear model	LP	ions
A1	0	–	B1	0	–
A2	−0.6197	0.6197	B2	−0.9841	0.9841
A3	−0.3066	0.3066	B3	−1.2086	1.2086
A4	−0.2011	0.2011	B4	−1.4309	1.4309

Total Energies and Binding Energies. The calculated TEs and BEs of cyclic and linear PEG in gas-phase or solvated models in the presence or absence of alkali metal ions are listed in Tables 2 and 3. The TEs in cyclic PEG are lower than in linear PEG in both the solvated and dry models in the presence or absence of metal ions, except in the case of Li^+, where linear PEG has lower energy. The calculations also show that the BEs are always higher in the presence of alkali metal ion. In the dry case, the BE trend in metal ions is $Li^+ > Na^+ > K^+$ in both linear and cyclic PEG. This indicates that smaller metal ions more easily form complexes with PEG without water. In solvated PEG, the BE trend in metal ions is reversed: $K^+ > Na^+ > Li^+$ in both linear and cyclic PEG. This is consistent with experimental findings[24] in the case of the linear PEG. Furthermore, without metal ions, cyclic PEG has slightly higher BE than linear PEG, but with metal ions cyclic PEG has a lower BE than linear PEG; the same trend is exhibited in all three cases: $K^+ > Na^+ > Li^+$. This implies that K^+ ion is highly preferred for complex formation with PEG compared with either Na^+ or Li^+ in water solution. We believe the calculated BEs and TEs for the PEG complexes are reasonably accurate, but no experimental data or higher-order theoretical values exist for direct comparison. The only existent estimate is the free energy between the bulk and the pore PEG−ion complex.[19] Our calculated BEs show that binding for the metal−PEG complexes is significantly stronger in the presence of water than in the gas phase. A more detailed examination of the role of solvation on the selectivity of metal ions also reveals the strong influence of water on the cation selectivity of PEG. PEG in the gas phase preferentially binds the small alkali metal cations relative to larger ones, but the opposite trend is observed in the solvated case. This finding agrees with some existing theoretical calculations[20,26,28] for cyclic PEG.

Partial Charge Distributions. The PC distribution is important for qualitative understanding of the structure and reactivity of molecules. An accurate PC distribution of a molecule is a vital ingredient for determining the intermolecular interactions. We start with the calculation of the effective charge Q* (eq 2 in section 3) and the PC (Δ*Q*) for every atom in the 24 PEG models. Figure 3 shows the data for Δ*Q* in

DOI: 10.1021/acs.jpca.7b04061
J. Phys. Chem. A 2017, 121, 4721−4731

Table 5. Net Partial Charges (PCs) in Different Structural Parts of Solvated Models

	PCs in structural units (electrons)				PCs in structural units (electrons)		
18c6 model	18c6	ions	water	linear model	LP	ions	water
A5	0.2041	–	−0.2041	B5	0.1466	–	−0.1466
A6	0.0438	1.7011	−1.7439	B6	−1.7789	1.8141	−0.0349
A7	0.1154	1.3777	−1.4933	B7	−1.8299	1.6220	0.2064
A8	0.2016	1.1632	−1.3707	B8	−1.7451	1.3202	0.4225

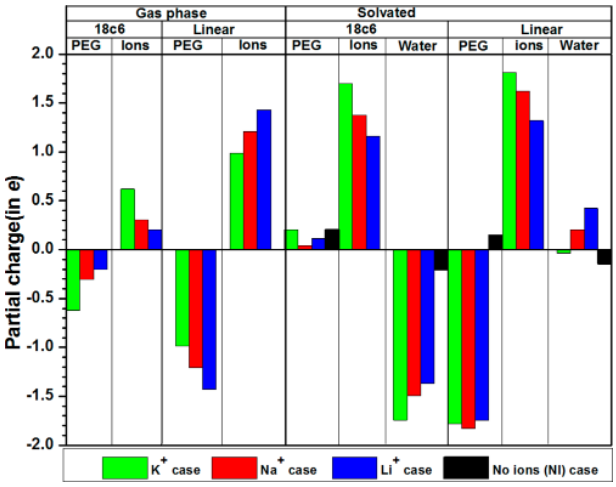

Figure 4. Calculated partial charge distributions on structural units of PEG, metal ion, and water in 18c6 and linear PEG for the dry case (left panel) and solvated model (right panel). The colors in the bars designate the type of metal ions (K^+, green; Na^+, red; Li^+, blue; no metal, black).

model A6 as an example. It should be noted that the ΔQ values for different atom types are not the same but depend on the local environment and bonding. For example, the atomic PCs of O and H in water are not the same as those in PEG. This clearly shows that the average charge transfers by O and H atoms in PEG are lower than those in water molecules. The calculations show that C and O atoms are electronegative but H and metal ion atoms are electropositive. By summing ΔQ for all of the atoms within each structural unit, we obtain the PC distributions for the PEG models listed in Tables 4 and 5. In order to illustrate the intricate pattern and subtle differences in PC distribution based on accurate ab initio evaluation, in Figure 4 we have plotted the results described above for better visual illustration. The figure shows that in the dry case, metal ions lose charge to PEG in both configurations, as expected. However, the trends in the sequence of K^+, Na^+, are Li^+ are opposite. In the crown form, the PCs of the metal ions decrease in the order $K^+ \rightarrow Na^+ \rightarrow Li^+$, whereas in the linear case, the PCs increase in the order $K^+ \rightarrow Na^+ \rightarrow Li^+$. In the solvated case of cyclic PEG, both PEG and metal ions lose charge to water. However, in the linear case, PEG also gains charge in the presence of metal ions but loses charge without metal ions. The metal ions always lose charge, as expected. Water molecules gain charge without ions but lose charge in the presence of Na^+ or Li^+, while gaining it slightly in the presence of K^+. In solvated models, cyclic PEG becomes electropositive for both cases with or without the metal ions. Linear PEG becomes electronegative in the presence of ions but electropositive in the absence of metal ions. This indicates that the solvation effect with metal ions has different characteristics of charge transfer for cyclic PEG versus linear PEG. The trend in the charge transfer in metal ions increases in the order of $Li^+ \rightarrow Na^+ \rightarrow K^+$ in both cyclic and linear PEG, which is also consistent with the trend in BE. Therefore, we note that the high-charge-transfer states of PEG can strongly bind solution cations. Finally, it should be noted that such detailed observations of partial charge distributions on PEG complexes would be very difficult to extract from experimental observations or from simulations using classical MD with parametrized force fields.

Total and Partial Bond Order Distribution. The influence of alkali metal bonding to PEG conformations is a subject of growing concern. In fact, the ion mobility experiment is not a viable option in providing the necessary evidence because of the complex and mixed influence of many competing factors. It appears that carefully controlled and accurate simulations are the only remaining option. The nature of interatomic bonding is an important component in determining the structure of PEG in different environments. Despite the generally acknowledged significance of the hydrogen bonding between PEG and water and assumed ionic bonding between metal ions and PEG, few studies have ever touched this subject in a detailed quantitative manner.

We have calculated the bond order (BO) values that quantify the strength of bonds between all pairs of atoms in the PEG models according to eq 2 (see section 3). We have also evaluated the total bond order (TBO) for all models and resolved them into partial bond orders (PBOs) for the individual structural units. The values are given in Tables 6 and 7. This new and somewhat unconventional approach has the merit of generalizing the bonding between individual atoms to that between different structural units in a simple and relatively transparent manner and reveals hidden details and

Table 6. Calculated Total Bond Orders (TBOs) and Partial Bond Orders (PBOs) between Different Structural Units of Gas-Phase Models of 18c6 and Linear PEG with Metal Ions

	structural units					structural units			
18c6 model	intra-18c6	18c6–I	I–I	TBO	linear model	intra-LP	LP–I	I–I	TBO
A1	15.3196	0.0000	0.0000	15.3196	B1	15.1856	0.0000	0.0000	15.1856
A2	15.5240	0.1496	0.0000	15.5405	B2	15.2859	0.0568	0.0000	15.3517
A3	15.4052	0.2175	0.2437	15.8664	B3	15.0697	0.2234	0.0000	15.2931
A4	15.3924	0.2628	0.2928	15.9480	B4	15.1914	0.5922	0.000	15.7836

DOI: 10.1021/acs.jpca.7b04061
J. Phys. Chem. A 2017, 121, 4721–4731

Table 7. Calculated Total Bond Orders (TBOs) and Partial Bond Orders (PBOs) between Different Structural Units of Solvated Models of 18c6 and Linear PEG with Metal Ions

	18c6 Models structural units					
model	intra-18c6	18c6–I	18c6–W	intra-W	W–I	TBO
A5	15.6016	0.0000	0.2485	119.9082	0.0000	135.7580
A6	15.6546	0.1926	0.1878	118.2489	0.1357	134.3410
A7	15.6708	0.2685	0.0972	118.2830	0.3333	134.6530
A8	15.6444	0.3745	0.0890	118.1982	o.4245	134.7305
	Linear PEG Models structural units					
model	intra-LP	LP–I	LP–W	intra-W	W–I	TBO
B5	15.5429	0.0000	0.1793	120.1132	0.0000	135.8358
B6	15.1803	0.0394	0.2191	120.3322	0.1869	135.9575
B7	15.1520	0.0755	0.1949	120.4835	0.4379	136.3441
B8	15.1639	0.0000	0.2327	120.4581	0.6662	136.5212

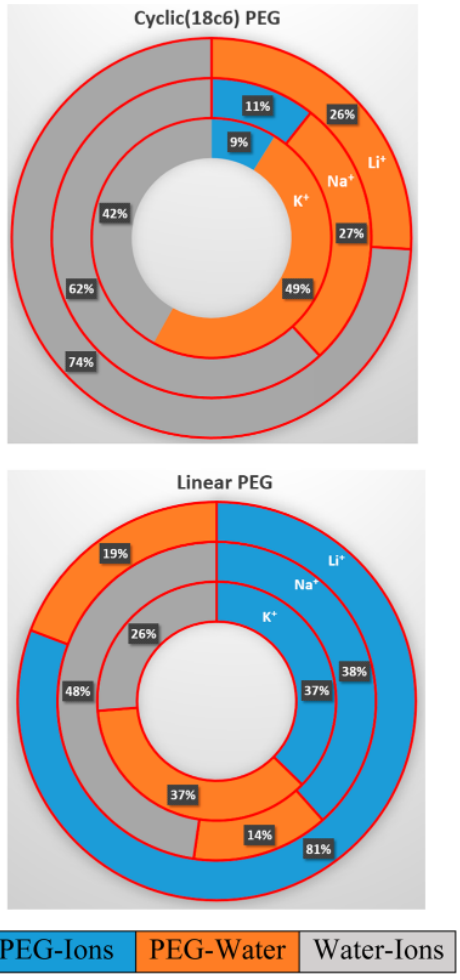

Figure 5. Multipie chart for percent contributions to TBO (HB + ionic bond) between different structural units (PEG–metal ions, blue; PEG–water, orange; water–metal ions, gray) for solvated 18c6 (top) and linear PEG (bottom). The widths of the rings for metal ions (K^+, Na^+, and Li^+) have no bearing on the quantitative meaning since the percent contributions are determined by the lengths of the circular sectors and are marked.

even surprising findings that few other approaches, be they experimental or computational, can disentangle. The TBO of cyclic PEG is larger than that of linear PEG in each pair of dry models, but the TBOs are smaller in solvated models. The PBO provides the information on the contribution from each structural unit in the system. In the dry case (Table 6), the PBOs within PEG are slightly higher in the cyclic than in the linear case. The PBO values between PEG and metal ions increase with decreasing size of the ion in both the cyclic and linear models. The results clearly show that bonding between ions (I–I) is completely absent in linear PEG models and with K^+ ions in the cyclic PEG models but is present for Na^+ and Li^+ ions in the cyclic models. In the solvated case (Table 7), there are three substantial types of interstructural bonding: PEG–ions, PEG–water and water–ions (W–I). These are vividly displayed in Figure 5. Bonding between PEG and ions is clearly the major contribution and increases with decreasing size of the metal ion in cyclic PEG but less so in the linear PEG. Conspicuously absent is the contribution from Li^+ ions, indicating that the Li^+ ions actually do not want to be close to each other. The W–I PBO values increase with decreasing size of the metal ion in both the cyclic and linear cases. The PBO values between PEG and water are less in the presence of metal ions and decrease with decreasing size of the ion in the cyclic case but in a random pattern for the linear case. Therefore, the bonding between PEG and water seems to be more complex. We believe that the proximity and orientation of water molecules also play a role in the bonding for the PEG complex. Hence, from the point view of TBO, linear PEG appears to have higher cohesion and stability than the cyclic PEG when solvated, a factor clearly related to the interaction with water molecules through hydrogen bonding.

Hydrogen Bonds and Metal Ion Interactions. We now focus on the nature of the HBs at the PEG–water interface and PEG–ion and water–ion bonds in solvated PEG models. We extracted the BO versus BL data for HBs in cyclic and linear PEG models, and they are displayed in Figure 6. Region I shows stronger HBs with larger BO values and region II much weaker HBs, including H···H bonds, in both cyclic and linear PEG. In the case of no metal ions, cyclic PEG has stronger O···H HBs than linear PEG (see Figure 6a). In the presence of metal ions (Figure 6b–d), linear PEG has stronger and somewhat more numerous HBs than cyclic PEG. Figure 7 shows the distribution of ionic bonds between metal ions and

DOI: 10.1021/acs.jpca.7b04061
J. Phys. Chem. A 2017, 121, 4721–4731

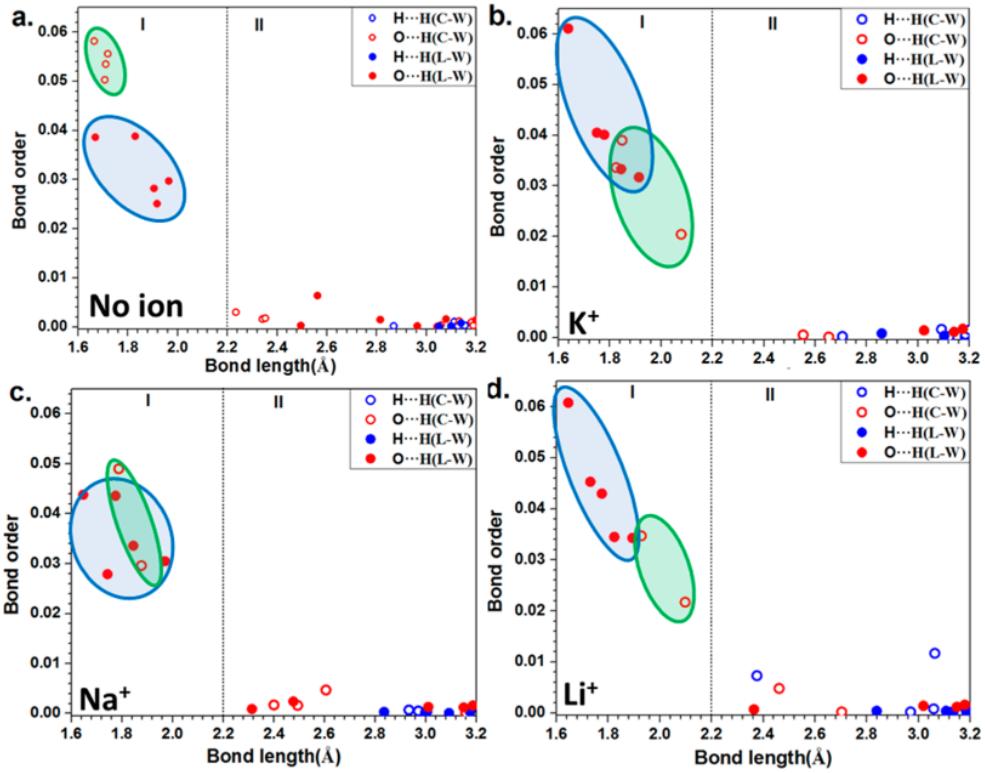

Figure 6. Comparison of hydrogen-bonding distribution between cyclic (open circles) and linear (solid circles) PEG (a) with no ion ions, (b) with K^+, (c) with Na^+, and (d) with Li^+. The shaded regions with color of green and blue are for strong hydrogen bonding in cyclic and linear PEG, respectively. Region I has stronger HBs, and region II has weaker HBs.

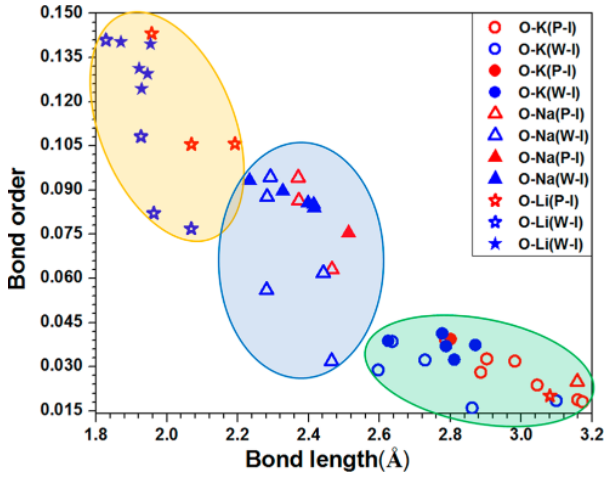

Figure 7. Bond order distribution of ionic bonds in solvated models of 18c6 and linear PEG. Each data point for a particular pair of bonding atoms is designated with a specific symbol and color. The open and solid symbols are for ionic bonding between O and ions in the cyclic and linear cases, respectively. The shaded regions with color of orange, blue, and green represent Li^+, Na^+, and K^+, respectively. The three oval-shaped regions are clearly separated.

O atoms in PEG and from water for both cyclic and linear PEG. The trend in the strength of ionic bonds is $Li^+ > Na^+ > K^+$ in both cyclic and linear PEG. In all cases, the ion−O bonds are shorter for O in water than O in PEG. The ionic bonds between metal ions and O atoms in PEG and water are more numerous in the cyclic PEG model if no metal ions are present, while the opposite is the case in the presence of metal ions. It is also clear that the number of ionic bonds is higher in cyclic PEG than in linear PEG. The ionic bonds between water and ions are more numerous than those between PEG and ions. The ionic bonds between PEG and ions decrease in the order $K^+ \rightarrow Na^+ \rightarrow Li^+$ in both cyclic and linear PEG but are completely absent for Li^+ ions in linear PEG. Figure 8 shows snapshots of the detailed geometries of relaxed positions of atoms in PEG and water forming ionic bonds in both cyclic and linear PEG. This contrasts with the ionic bond distributions for the two topologies of PEG in the presence of K^+, Na^+, and Li^+. The numbers of metal ionic bonds are in the order of K−O > Na−O > Li−O in the cyclic PEG model. For linear PEG, the trend of metal ion bonds is opposite to the cyclic PEG trend, since smaller ions have stronger interactions with solvent molecules than with PEG and it is harder to trap the ion to the chain. These results suggests that the small metal ion (Li^+) has difficulty in forming a complex with the PEG chain. In other words, PEG is more effective in forming complexes with larger cations.

Effects of Chain Size on PEG Properties. To examine the effects on the electronic properties in the case of a longer chain, simulations were carried out on eight additional models including alkali ions in the presence or absence of water (C1−C8 in Table 1, illustrated in Figure 2f,g). Those models are exactly double in each type of atom compared with models B1−B8, making it easier to compare with the other models simultaneously. The results with the longer chains are listed in Tables S1−S3 in the Supporting Information. These additional calculations show that the results with the longer chain are only slightly different from those with the short chain and that the

DOI: 10.1021/acs.jpca.7b04061
J. Phys. Chem. A 2017, 121, 4721−4731

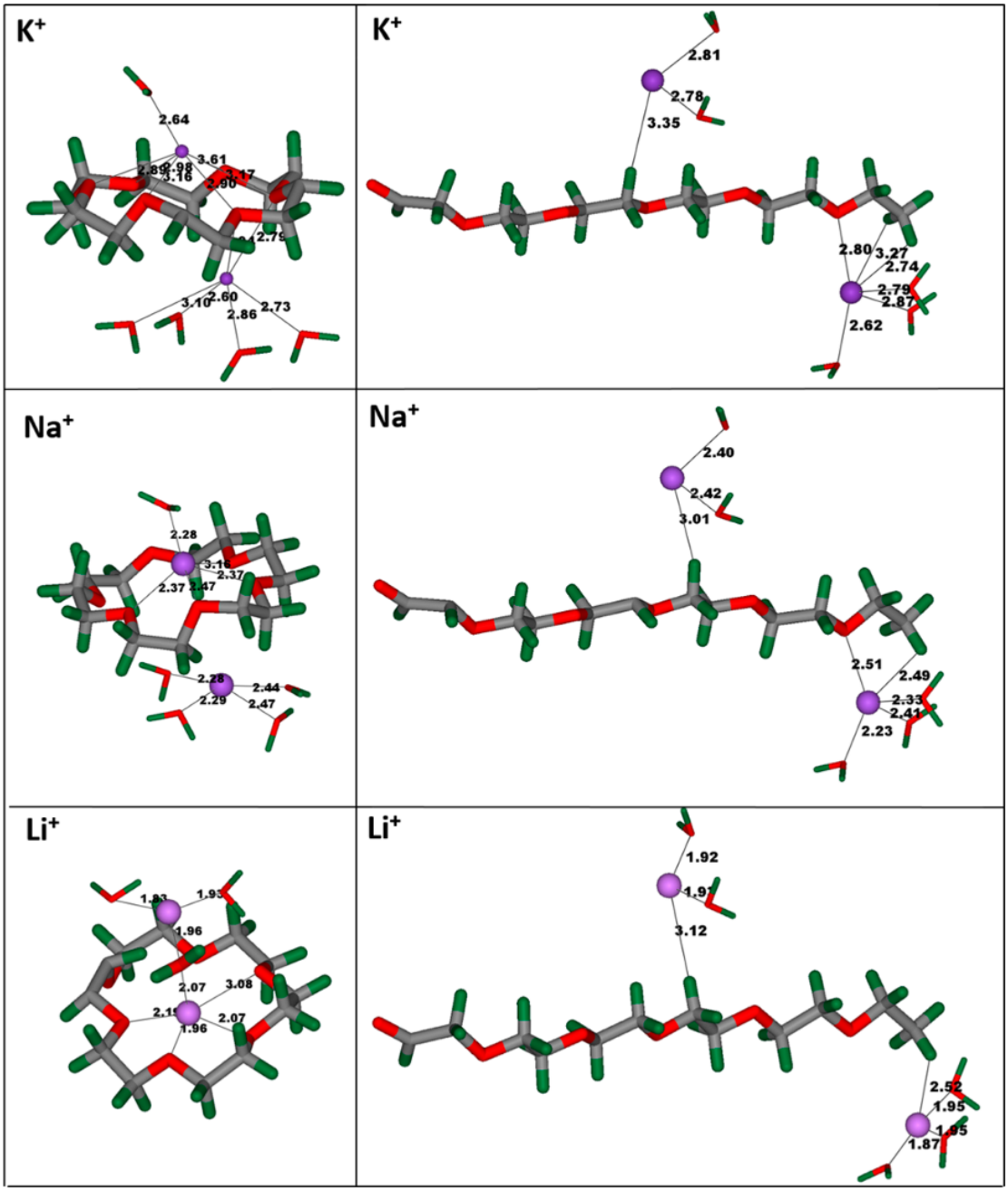

Figure 8. Snapshots of the geometric locations of metal ions from the nearest O atoms in PEG or relevant water molecules. Other water molecules have been removed for clarity. The left panel is for the solvated cyclic (18c6) model and the right panel for the linear PEG model. The metal ions present are K^+, Na^+, and Li^+ from top to bottom.

longer chain basically does not alter any of the observations presented above. This includes the trends in binding energies, PC distributions, and PBO values in both the dry and solvated cases. The minor differences may arise from the variation in the molar mass of linear PEG or local distributions of water and ions in the system.

5. SUMMARY AND CONCLUSIONS

In conclusion, we have presented a comprehensive study of the electronic structure and bonding properties of PEG complexes, including the effects of water and alkali ions, motivated by the puzzling experimentally observed behavior of PEG in aqueous solutions. We have performed massive ab initio calculations to study the properties of small cyclic and linear PEG polymers in aqueous solutions, either in vacuo or with 200 explicit water molecules and alkali metal ions. We designed 24 different fully relaxed atomistic models of PEG in the cyclic crown ether configuration and in linear chain configurations with two different numbers of monomer units to analyze the binding energy, partial charge distribution, and interatomic bonding of this complex molecular system in different molecular environments. Our detailed pairwise comparisons between the

DOI: 10.1021/acs.jpca.7b04061
J. Phys. Chem. A 2017, 121, 4721−4731

quantitative measures of binding energy, partial charge, and atomic hydrogen bonding and ionic bonding provide specific answers to specific questions about the stability and nature of PEG in aqueous solutions.

The following are specific conclusions of our work: (1) In the solvated PEG, the BE trend for metal ions is $K^+ > Na^+ > Li^+$, consistent with experimental findings. (2) Cyclic PEG has larger BE than linear PEG in vacuo, except in the presence of Li^+. (3) In pure solvent with no alkali ions, cyclic PEG has a slightly higher BE than linear PEG. (4) In the aqueous solution with alkali ions, both cyclic PEG and metal ions lose charge to water, whereas in linear PEG, water gains charge only in the case of K^+ ion but loses charge in the case of Na^+ and Li^+ ions. (5) The nature of charge transfer depends upon the PEG conformation, type of ions, and presence or absence of explicit solvent. The trends for charge transfer for metal ions and water are opposite for the two forms of PEG in vacuo. (6) There are significant differences in HB and ionic bond distributions between cyclic and linear PEGs and between different metal ions. In the case of no metal ions, cyclic PEG has stronger O···H HBs than linear PEG. With metal ions, linear PEG has stronger and somewhat more HBs than cyclic PEG. (7) The analysis of BO values of HB at the PEG−water interface is complicated because of the interrelatedness of different effects, and the ab initio calculation is the only way to distinguish between them.

Our results show that the interactions of alkali ions with PEG are enhanced by the presence of explicit solvent, leading to charge separation, effectively conferring positive partial charge to cyclic PEG and stronger negative partial charge to linear PEG. It should not be difficult to detect this effect experimentally. As this effect depends essentially on the detailed molecular environment, the notion of "charged PEG states" has no general meaning. Accurate determination of the partial charge distribution of PEG can play a significant role in predicting interactions with other biomolecular entities such as ligands, proteins, membrane channels, or drugs. Detailed analysis of different types of bonding provides an in-depth understanding of the dynamic interplay of different types of atoms and bonds in PEG in different molecular environments. The present effort demonstrates that advanced computational studies can go beyond what is available from classical or semiclassical descriptions of large complex biomolecular systems with explicit solvent effects. It is obvious that the present method and approach can be applied to the situation with the presence of anions such as F^- or Cl^- or divalent metal ions such has Mg^{2+} or Ca^{2+} as long as the goal of the study is well-defined and focused. The only limitation is the availability of the computational resources if it requires much larger cells, especially in the solvated model.

ASSOCIATED CONTENT

Supporting Information

The Supporting Information is available free of charge on the ACS Publications website at DOI: 10.1021/acs.jpca.7b04061.

Total energies, binding energies, partial charges, and total and partial bond orders in longer (n = 12) linear PEG (LP-12) models (PDF)

AUTHOR INFORMATION

Corresponding Author

*E-mail: chingw@umkc.edu. Phone: +1 (816) 235-2503.

ORCID

Wai-Yim Ching: 0000-0001-7738-8822

Author Contributions

R.P. suggested the topic. W-Y.C. and L.P. initiated the project. L.P. did the calculations. All of the authors participated in the discussion of the results and wrote, edited, and proofread the manuscript.

Notes

The authors declare no competing financial interest.

ACKNOWLEDGMENTS

L.P. was supported by a research grant from the School of Graduate Studies at UMKC. R.P. acknowledges the financial support from the Slovenian Research Agency (research core funding, no. P1-0055). This research used the resources of NERSC supported by the Office of Science of DOE under Contract DE-AC03-76SF00098 and the computing resources of the Bioconsortium of the University of Missouri.

REFERENCES

(1) Woodle, M. C.; Lasic, D. D. Sterically Stabilized Liposomes. *Biochim. Biophys. Acta, Rev. Biomembr.* **1992**, *1113*, 171.

(2) Bekiranov, S.; Bruinsma, R.; Pincus, P. Solution Behavior of Polyethylene Oxide in Water as a Function of Temperature and Pressure. *Phys. Rev. E: Stat. Phys., Plasmas, Fluids, Relat. Interdiscip. Top.* **1997**, *55*, 577.

(3) Devanand, K.; Selser, J. Asymptotic Behavior and Long-Range Interactions in Aqueous Solutions of Poly (ethylene oxide). *Macromolecules* **1991**, *24*, 5943.

(4) Israelachvili, J. The Different Faces of Poly (ethylene glycol). *Proc. Natl. Acad. Sci. U. S. A.* **1997**, *94*, 8378.

(5) Templeton, N. S. *Gene and Cell Therapy: Therapeutic Mechanisms and Strategies*; CRC Press: Boca Raton, FL, 2015.

(6) Li, L.; Kantor, A.; Warne, N. Application of a PEG Precipitation Method for Solubility Screening: A Tool for Developing High Protein Concentration Formulations. *Protein Sci.* **2013**, *22*, 1118.

(7) McPherson, A.; Gavira, J. A. Introduction to Protein Crystallization. *Acta Crystallogr., Sect. F: Struct. Biol. Commun.* **2014**, *70*, 2.

(8) Strey, H. H.; Podgornik, R.; Rau, D. C.; Parsegian, V. A. DNA-DNA Interactions. *Curr. Opin. Struct. Biol.* **1998**, *8*, 309.

(9) Cohen, J.; Podgornik, R.; Hansen, P. L.; Parsegian, V. A. A Phenomenological One-Parameter Equation of State for Osmotic Pressures of PEG and Other Neutral Flexible Polymers in Good Solvents. *J. Phys. Chem. B* **2009**, *113*, 3709.

(10) Kjellander, R.; Florin, E. Water Structure and Changes in Thermal Stability of The System Poly (ethylene oxide)−Water. *J. Chem. Soc., Faraday Trans. 1* **1981**, *77*, 2053.

(11) Robertson, J. W.; Rodrigues, C. G.; Stanford, V. M.; Rubinson, K. A.; Krasilnikov, O. V.; Kasianowicz, J. J. Single-Molecule Mass Spectrometry in Solution Using a Solitary Nanopore. *Proc. Natl. Acad. Sci. U. S. A.* **2007**, *104*, 8207.

(12) Rubinson, K. A.; Krueger, S. Poly (ethylene glycol)s 2000−8000 in Water may be Planar: A Small-Angle Neutron Sattering (SANS) Structure Study. *Polymer* **2009**, *50*, 4852.

(13) Krongsuk, S.; Kerdcharoen, T.; Hannongbua, S. The Hydration Structure of 18-crown-6/K^+ Complex as Studied by Monte Carlo Simulation using Ab Initio Fitted Potential. *J. Mol. Graphics Modell.* **2006**, *25*, 55.

(14) Lee, H.; de Vries, A. H.; Marrink, S.-J.; Pastor, R. W. A Coarse-Grained Model for Polyethylene Oxide and Polyethylene Glycol: Conformation and Hydrodynamics. *J. Phys. Chem. B* **2009**, *113*, 13186.

(15) Magarkar, A.; Karakas, E.; Stepniewski, M.; Róg, T.; Bunker, A. Molecular Dynamics Simulation of PEGylated Bilayer Interacting with Salt Ions: A Model of the Liposome Surface in the Bloodstream. *J. Phys. Chem. B* **2012**, *116*, 4212.

DOI: 10.1021/acs.jpca.7b04061
J. Phys. Chem. A 2017, 121, 4721−4731

(16) Uematsu, Y. Electrophoresis of Electrically Neutral Porous Spheres Induced by Selective Affinity of Ions. *Phys. Rev. E* **2015**, *91*, 022303.
(17) McDaniel, J. G.; Choi, E.; Son, C.-Y.; Schmidt, J.; Yethiraj, A. Conformational and Dynamic Properties of Poly (ethylene oxide) in an Ionic Liquid: Development and Implementation of a First-Principles Force Field. *J. Phys. Chem. B* **2016**, *120*, 231.
(18) Tasaki, K. Poly (oxyethylene)−Cation Interactions in Aqueous Solution: A Molecular Dynamics Study. *Comput. Theor. Polym. Sci.* **1999**, *9*, 271.
(19) Balijepalli, A.; Robertson, J. W.; Reiner, J. E.; Kasianowicz, J. J.; Pastor, R. W. Theory of Polymer−Nanopore Interactions Refined Using Molecular Dynamics Simulations. *J. Am. Chem. Soc.* **2013**, *135*, 7064.
(20) Guo, X.; Zhu, Y.; Wei, M.; Wu, X.; Lu, L.; Lu, X. Theoretical Study of Hydration Effects on the Selectivity of 18-Crown-6 between K^+ and Na^+. *Chin. J. Chem. Eng.* **2011**, *19*, 212.
(21) Aksoyoglu, M. A.; Podgornik, R.; Bezrukov, S. M.; Gurnev, P. A.; Muthukumar, M.; Parsegian, V. A. Size-Dependent Forced PEG Partitioning into Channels: VDAC, OmpC, and α-Hemolysin. *Proc. Natl. Acad. Sci. U. S. A.* **2016**, *113*, 9003.
(22) Reiner, J. E.; Kasianowicz, J. J.; Nablo, B. J.; Robertson, J. W. Theory for Polymer Analysis Using Nanopore-Based Single-Molecule Mass Spectrometry. *Proc. Natl. Acad. Sci. U. S. A.* **2010**, *107*, 12080.
(23) Rodrigues, C. G.; Machado, D. C.; Chevtchenko, S. F.; Krasilnikov, O. V. Mechanism of KCl Enhancement in Detection of Nonionic Polymers by Nanopore Sensors. *Biophys. J.* **2008**, *95*, 5186.
(24) Breton, M. F.; Discala, F.; Bacri, L.; Foster, D.; Pelta, J.; Oukhaled, A. Exploration of Neutral Versus Polyelectrolyte Behavior of Poly (ethylene glycol)s in Alkali Ion Solutions using Single-Nanopore Recording. *J. Phys. Chem. Lett.* **2013**, *4*, 2202.
(25) Glendening, E. D.; Feller, D. An Ab Initio Investigation of the Structure and Alkaline Earth Divalent Cation Selectivity of 18-Crown-6. *J. Am. Chem. Soc.* **1996**, *118*, 6052.
(26) Glendening, E. D.; Feller, D.; Thompson, M. A. An Ab Initio Investigation of the Structure and Alkali Metal Cation Selectivity of 18-Crown-6. *J. Am. Chem. Soc.* **1994**, *116*, 10657.
(27) Martínez-Haya, B.; Hurtado, P.; Hortal, A. R.; Hamad, S.; Steill, J. D.; Oomens, J. Emergence of Symmetry and Chirality in Crown Ether Complexes with Alkali Metal Cations. *J. Phys. Chem. A* **2010**, *114*, 7048.
(28) More, M. B.; Ray, D.; Armentrout, P. B. Intrinsic Affinities of Alkali Cations for 15-Crown-5 and 18-Crown-6: Bond Dissociation Energies of Gas-Phase M^+ Crown Ether Complexes. *J. Am. Chem. Soc.* **1999**, *121*, 417.
(29) Hohenberg, P.; Kohn, W. Inhomogeneous Electron Gas. *Phys. Rev.* **1964**, *136*, B864.
(30) Kohn, W.; Sham, L. J. Self-Consistent Equations Including Exchange and Correlation Effects. *Phys. Rev.* **1965**, *140*, A1133.
(31) Jorgensen, W. L.; Chandrasekhar, J.; Madura, J. D.; Impey, R. W.; Klein, M. L. Comparison of Simple Potential Functions for Simulating Liquid Water. *J. Chem. Phys.* **1983**, *79*, 926.
(32) Pettersen, E. F.; Goddard, T. D.; Huang, C. C.; Couch, G. S.; Greenblatt, D. M.; Meng, E. C.; Ferrin, T. E. UCSF Chimera□ a Visualization System for Exploratory Research and Analysis. *J. Comput. Chem.* **2004**, *25*, 1605.
(33) Kresse, G.; Furthmüller, J. Efficient iterative schemes for *ab initio* total-energy calculations using a plane-wave basis set. *Phys. Rev. B: Condens. Matter Mater. Phys.* **1996**, *54*, 11169.
(34) Perdew, J. P.; Burke, K.; Ernzerhof, M. Generalized Gradient Approximation Made Simple. *Phys. Rev. Lett.* **1996**, *77*, 3865.
(35) Adhikari, P.; Wen, A. M.; French, R. H.; Parsegian, V. A.; Steinmetz, N. F.; Podgornik, R.; Ching, W.-Y. Electronic Structure, Dielectric Response, and Surface Charge Distribution of RGD (1FUV) Peptide. *Sci. Rep.* **2015**, *4*, 5605.
(36) Poudel, L.; Rulis, P.; Liang, L.; Ching, W.-Y. Electronic Structure, Stacking Energy, Partial Charge, and Hydrogen Bonding in Four Periodic B-DNA Models. *Phys. Rev. E* **2014**, *90*, 022705.
(37) Poudel, L.; Steinmetz, N. F.; French, R. H.; Parsegian, V. A.; Podgornik, R.; Ching, W.-Y. Implication of the Solvent Effect, Metal Ions and Topology in the Electronic Structure and Hydrogen Bonding of Human Telomeric G-quadruplex DNA. *Phys. Chem. Chem. Phys.* **2016**, *18*, 21573.
(38) Poudel, L.; Wen, A. M.; French, R. H.; Parsegian, V. A.; Podgornik, R.; Steinmetz, N. F.; Ching, W. Y. Electronic Structure and Partial Charge Distribution of Doxorubicin in Different Molecular Environments. *ChemPhysChem* **2015**, *16*, 1451.
(39) Ching, W.-Y.; Rulis, P. *Electronic Structure Methods for Complex Materials: The Orthogonalized Linear Combination of Atomic Orbitals*; Oxford University Press: Oxford, U.K., 2012.
(40) Adhikari, P.; Xiong, M.; Li, N.; Zhao, X.; Rulis, P.; Ching, W.-Y. Structure and Electronic Properties of a Continuous Random Network Model of an Amorphous Zeolitic Imidazolate Framework (a-ZIF). *J. Phys. Chem. C* **2016**, *120*, 15362.
(41) Baral, K.; Adhikari, P.; Ching, W. Y. Ab Initio Modeling of the Electronic Structures and Physical Properties of a-$Si_{1-x}Ge_xO2$ Glass (x= 0 to 1). *J. Am. Ceram. Soc.* **2016**, *99*, 3677.
(42) Ching, W. Theoretical Studies of the Electronic Properties of Ceramic Materials. *J. Am. Ceram. Soc.* **1990**, *73*, 3135.
(43) Liang, L.; Rulis, P.; Kahr, B.; Ching, W. Theoretical Study of the Large Linear Dichroism of Herapathite. *Phys. Rev. B: Condens. Matter Mater. Phys.* **2009**, *80*, 235132.
(44) Eifler, J.; Podgornik, R.; Steinmetz, N. F.; French, R. H.; Parsegian, V. A.; Ching, W.-Y. Charge Distribution and Hydrogen Bonding of a Collagen α2-Chain in Vacuum, Hydrated, Neutral, and Charged Structural Models. *Int. J. Quantum Chem.* **2016**, *116*, 681.
(45) Mulliken, R. S. Electronic Population Analysis on LCAO−MO Molecular Wave Functions. I. *J. Chem. Phys.* **1955**, *23*, 1833.

DOI: 10.1021/acs.jpca.7b04061
J. Phys. Chem. A 2017, 121, 4721−4731